On Estimation of Numerical Solution in Prager&Synge Sense

Alekseev A.K.[1[0000-0001-8317-8688]], Bondarev A.E.[2[0000-0003-3681-5212]]

[1]RSC Energia, Korolev, Russia

[2]Keldysh Institute of Applied Mathematics RAS, Moscow, Russia

bond@keldysh.ru

Abstract. The numerical solution in sense of Prager&Synge is defined as a hypersphere containing a true solution of a system of partial differentiation equations (PDE). In the original variant Prager&Synge method is based on special orthogonal properties of PDE and may be applied only to several equations. Herein, the Prager&Synge solution (center and radius of the hypersphere) is estimated using the ensemble of numerical solutions obtained by independent algorithms. This approach is not problem dependent and may be applied to arbitrary system of PDE. Several options for computation of the Prager&Synge solution are considered. The first one is based on the search for the orthogonal truncation errors and their transformation. The second is based on the orthogonalization of approximation errors obtained using the defect correction method. It applies the superposition of numerical solutions. The third option uses the width of the ensemble of numerical solutions. The numerical tests for the two dimensional inviscid flows are presented that demonstrate the acceptable effectivity of the approximation error estimates based on the solution in the Prager&Synge sense.

Keywords: Prager&Synge method, a posteriori error estimation, ensemble of numerical solutions.

1 Introduction

We discuss a notion of numerical solution in the sense of Prager&Synge (some hypersphere containing the true solution) from the viewpoint of the approximation error estimation that is the necessary component of the verification of numerical solutions. The verification of the numerical solution is required by the modern standards [1,2] and is based on the *a priori* and *a posteriori* error estimates. The Prager&Synge method [3,4,5] is historically the first approach to *a posteriori* error estimation, unfortunately, highly underestimated. Below we consider an universal version of this method, using notations that follows. $A_h u_h = \rho_h$ is a discrete approximation of a system of partial differential equations, $u_h \in R^M$ denotes the numerical solution

ICCS Camera Ready Version 2024
To cite this paper please use the final published version:
DOI: 10.1007/978-3-031-63783-4_24

(grid function), $\tilde{u}_h \in R^M$ is the projection of a true solution onto the considered grid, $\Delta\tilde{u}_h = u_h - \tilde{u}_h$ is the approximation error, Δu_h is an estimate of the approximation error.

A priori error estimates have the form $\left\|\Delta\tilde{u}_h\right\| \le Ch^n$ (n is the order of approximation, h is a grid step). These estimates describe the properties of the algorithm and do not depend on the specific solution. Unfortunately, the unknown constant C restricts the practical applications of this approach.

A posteriori error estimate has the form $\left\|\Delta\tilde{u}_h\right\| \le I(u_h)$ defined by a computable error indicator $I(u_h)$, which depends on the concrete numerical solution u_h and has no unknown constants. The main domain of *a posteriori* error estimation is related with the finite-element analysis [3-8]. For the problems governed by the equations of the hyperbolic or mixed type (typical CFD problems), the progress in the *a posteriori* error estimation is limited. The standards [1,2] recommend the Richardson extrapolation (RE) [9,10,11] for the approximation error estimation. However, for the compressible flows, the application of standard RE is impossible due to the absence of the global convergence order [12]. The generalized Richardson extrapolation (GRE) [10,11] provides an estimate for the spatial distribution of the convergence order. Unfortunately, GRE demonstrates the high computational burden since it requires at least four consequent refinement of the mesh.

Thus, the computationally inexpensive *a posteriori* error estimators are of current interest in the CFD domain. By this reason we consider, herein, the famous Prager&Synge [3,4,5] method, which seems to be highly underestimated both from the viewpoint of general idea and from the viewpoint of applicability domain. The new options are considered that realize the solution in the sense of Prager&Synge (a hypersphere containing the projection of the true solution on computational grid).

As the first option, we construct an artificial approximation error using the estimate of the truncation errors performed by forward postprocessor and the estimate of the approximation error by an adjoint postprocessor.

As the second option, we construct an artificial solution by the superposition of numerical solutions (obtained by independent algorithms) that provides the approximation error, orthogonal to the error of certain analyzed solution.

Both these options are intrusive and are implemented by rather complex algorithms.

As the third option, we apply the method based on the width of the ensemble of solutions ([14]), which may be considered as some nonintrusive approximation of the version of the Prager@Synge method, based on the superposition of solutions.

The two-dimensional compressible flows, governed by the Euler equations, are used in the numerical tests in order to compare the above mentioned algorithms. The error estimates by modified Prager&Synge are compared with the “true” discretization errors obtained by subtracting the analytical solutions from the numerical solutions.

ICCS Camera Ready Version 2024
To cite this paper please use the final published version:
DOI: 10.1007/978-3-031-63783-4_24

2 Prager&Synge method

The “hypercircle method” by Prager@Synge [3,4,5] is the oldest algorithm for *a posteriori* error estimation. At present, the term "hypercircle" is used in distant science domains, so, in order to avoid confusion, we mark this method as the "Prager&Synge method". We provide herein some presentation of the original Prager&Synge method with illustrations and citations.

Initially, the Prager&Synge method was applied for the solution of the Poisson equation

$$\nabla^2 u = \rho\,,\ u_\Gamma = f\,. \tag{1}$$

Two additional linear subspaces of functions are used:

-the subspace of gradients $\partial v/\partial x_i$ ($v \in H^1$) with boundary conditions $v_\Gamma = f$,

-the subspace of functions $q \in H^1$, such that $div(q) = \rho$.

The following orthogonality condition is valid for these functions ($\tilde{u}$ is the exact solutions of the Poisson equation)

$$((\nabla v - \nabla\tilde{u}),(q - \nabla\tilde{u})) = 0\,. \tag{2}$$

Usually v is assumed to be a numerical solution u_h. The scalar products and norms correspond to L_2 and its finite-dimensional analogue.

The orthogonality relation (Eq. (2)) engenders the inequality for the approximation error, since the leg of a right triangle is less the hypotenuse

$$\left\|\nabla(\tilde{u} - u_h)\right\| \le \left\|\nabla u_h - q\right\|\,. \tag{3}$$

So, the Prage@Synge method provides *a posteriori* error estimation from purely geometrical ideas without unknown constants. Since we are unable to compete with authors of the method in vividness, we provide the citation from [5]:

“Imagine a flat piece of country. Imagine in it two strait narrow roads which intersect at right angles. Imagine two blind men set down by helicopter, one on each road. Provide them with a long measuring tape, stretching from the one man to the other man. Let the tape be embossed, so they can read it, even though blind. Without moving, let them tighten the tape and read it. Suppose it reads 100 yards apart.

We are to ask each of them how far he is from the cross roads.

These men, though blind, are very intelligent, and they know, that the hypotenuse of a right-angled triangle is greater than either the other two sides. So each of the men says that his distance from the cross-roads is less than (or possible equal to) 100 yards”.

Fig. 1 provides the illustration from [5] for this “Two blind men” problem.

ICCS Camera Ready Version 2024
To cite this paper please use the final published version:
DOI: 10.1007/978-3-031-63783-4_24

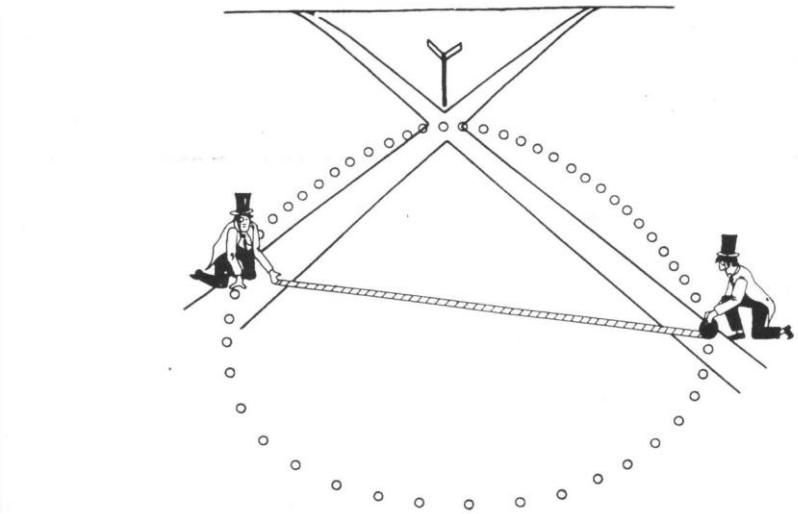

Fig. 1. "Two blind men and their hypercircle [5]"

Unfortunately, the classic variant of the Prager&Synge method has significant restrictions:

it may be applied to rather narrow domain of equations (Poisson equation, biharmonic equation), which does not include such equations as Euler on Navier-Stokes,

it provides the norm of the error of the solution gradient (Eq. 3) and is unable to estimate the norm $\|\tilde{u} - u_h\|$ of the solution error, which is of the primal interest in practice**.**

Below we try to demonstrate that the method by Prager&Synge may be significantly modified to avoid these restrictions.

3 The numerical solution in Prager&Synge sense

The main (and underestimated) idea by Prager&Synge consists in the original concept of the numerical solution. We designate it as the numerical solution in the Prager&Synge sense.

The numerical solution, defined by the standard way, is considered to be an element of the sequence of solutions u_{h_m} at refining grids (grid step $h_m \to 0$ at $m \to \infty$) that is assumed to converge to the exact solution $u_{h_m} \to \tilde{u}_{h_m}$. The mesh adaptation and refinement are the key elements enabling the success of this approach.

In contrast, Synge stated ([4], p. 97): *" In general,* ***a limiting process is not used, and we do not actually find the solution....*** *But although we do not find it, we learn something about its position, namely, that it is located on a certain hypercircle in function space".*

ICCS Camera Ready Version 2024
To cite this paper please use the final published version:
DOI: 10.1007/978-3-031-63783-4_24

In the finite-dimensional case the hyprecircle by Prager&Synge is equivalent to the hypersphere. So, the numerical solution in sense of Prager&Synge may be defined as a hypersphere with the center

$$C_h = u_h \tag{4}$$

and a radius R_h

$$\left\| \tilde{u}_h - C_h \right\| \le R_h . \tag{5}$$

This hypersphere contains the true solution.

Equations (4),(5) demonstrated that the numerical solution by Prager&Synge is naturally related with the *a posteriori* error estimation. In the contrast to the standard approach to approximation, a convergence of numerical solution is not obligatory. The mesh refinement is not mandatory also and should be performed only if the magnitude of R_h is not acceptable from the viewpoint of practical needs (that may be checked using Cauchy–Bunyakovsky–Schwarz inequality for valuable functionals (for example, [14])). In this way, the natural stopping criterion for the mesh refinement termination may be stated. So, the solution in sense of Prager&Synge is free from the "tyranny" of the mesh refinement and adaptation that governs the modern CFD applications.

Unfortunately, the standard domain of the Prager&Synge method applicability is very narrow. Fortunately, the domain of the Prager&Synge method applicability may be extended to an arbitrary PDE system that we try to show.

In the spirit of the Prager&Synge solution we search for an auxiliary solution $u_\perp$ such that

$$(u_h^{(i)} - \tilde{u}_h, u_\perp - \tilde{u}_h)_\Omega = (\Delta\tilde{u}_h^{(i)}, \Delta\tilde{u}_\perp)_\Omega = 0 . \tag{6}$$

If the auxiliary solution $u_\perp$ is determined, the numerical solution in the Prager&Synge sense is defined, since $\left\| u_h^{(i)} - \tilde{u}_h \right\| \le \left\| u_h^{(i)} - u_\perp \right\|$ and the centre and the radius of the hypersphere containing the true solution are determined.

4 The methods for approximation of Prager&Synge solution

We consider several algorithms for calculation of the Prager&Synge numerical solutions. In general, all of them are based on the usage of the ensemble of numerical solutions obtained by independent algorithms. The main differences between these algorithms concern their computational complexity.

ICCS Camera Ready Version 2024
To cite this paper please use the final published version:
DOI: 10.1007/978-3-031-63783-4_24

4.1. Truncation error based estimation of Prager&Synge solution

Truncation errors $\delta u_h^{(i)}$ may be estimated either by the differential approximation [18] or by the special postprocessor [19] acting on the numerical solution. Numerical tests [14,17] demonstrate that the truncation errors $\delta u_h^{(i)}$ on the ensemble of independent solutions are close to orthogonal. The approximation error $\Delta u_h^{(i)}$ may be estimated using the truncation error by solving a special problem for disturbances (see for instance [20])

$$\Delta u_h^{(i)} = A_h^{-1} \delta u_h^{(i)} . \tag{7}$$

However, it is more interesting to express the orthogonality condition (Eq. (6)) in terms of nonintrusively computable truncation errors. Let's select some vector $\theta \perp \delta u_h^{(i)}$ and transform it using forward and adjoint operators:

$$\delta u_\perp = A_h A_h^* \theta . \tag{8}$$

Expression (8) may be inverted to obtain

$$\theta = A_h^{-1*} A_h^{-1} \delta u_\perp . \tag{9}$$

The orthogonality condition $\theta \perp \delta u_h^{(i)}$ is equivalent to relation (6) since

$$(\delta u_h^{(i)}, \theta)_\Omega = (\delta u_h^{(i)}, A_h^{-1*} A_h^{-1} \delta u_\perp)_\Omega = (A_h^{-1} \delta u^{(i)}, A_h^{-1} \delta u_\perp)_\Omega = (\Delta u_h^{(i)}, \Delta u_\perp)_\Omega = 0 . \tag{10}$$

Finally

$$\Delta u_\perp = A_h^{-1} \delta u_\perp = A_h^* \theta . \tag{11}$$

Equation (11) demonstrates that $\Delta u_\perp$ may be computed nonintrusively using the adjoint postprocessor that implements the solution of adjoint problem (similarly to [16,19]).

The search for $\theta \perp \delta u_h^{(i)}$ may be conducted as follows:

1. By choice of arbitrary $\theta \perp \delta u_h^{(i)}$ (under condition $\|\theta\| = \|\delta u_h^{(i)}\|$).
2. By selection of θ that is equal to the truncation error of an additional numerical solution

ICCS Camera Ready Version 2024
To cite this paper please use the final published version:
DOI: 10.1007/978-3-031-63783-4_24

$$\theta = \delta u_h^{(k)}. \tag{12}$$

The latter option is caused by the numerical tests [17] that demonstrate the truncation errors, corresponding to independent algorithms, to be close to orthogonal.

If $\delta u_\perp = A_h A_h^* \theta$ is available, we may compute the auxiliary solution by the defect correction approach

$$u_\perp = A^{-1}(\rho + \delta u_\perp). \tag{13}$$

It enables to obtain the inequality

$$\left\| u_h^{(k)} - \tilde{u} \right\| \le \left\| u_h^{(k)} - u_\perp \right\| = R_h. \tag{14}$$

The centre $C_h = u_h^{(k)}$ and radius $R_h = \left\| u_h^{(k)} - u_\perp \right\|$ determine the numerical solution in the sense of the Prager&Synge.

Unfortunately, this algorithm (Eqs. (8)-(14)) is extremely complicated from the algorithmic viewpoint (mainly due to the application of the adjoint solver) and unstable (due to the differentiation of a non regular function by the adjoint solver). The numerical tests demonstrated highly pessimistic estimations (too great estimates of the error norm), so, the above discussion is mainly of the heuristic value and illustrates the existence of auxiliary solution $u_\perp$ that determines the solution in sense of Prager&Synge.

4.2. Approximation error based estimation of the solution in Prager&Synge sense

We may construct the auxiliary solution $u_\perp$ in another way using the superposition of N numerical solutions (obtained by independent algorithms on the same grid)

$$u_\perp = \sum_{i=1}^{N} w_i u_h^{(i)} = w_i u_h^{(i)}, \tag{15}$$

$$\sum_{i=1}^{N} w_i = 1. \tag{16}$$

First, we select some basic numerical solution $u_h^{(0)}$ (centre of the hypersphere) and estimate corresponding approximation error $\Delta u_h^{(0)} = A_h^{-1} \delta u_h^{(0)} \approx \Delta \tilde{u}_h^{(0)} = u_h^{(0)} - \tilde{u}_h$ using the defect correction approach. Second, we search for the auxiliary solution $u_\perp$ that is defined by the approximation error $\Delta u_\perp$ orthogonal to the error of the basic numerical solution

ICCS Camera Ready Version 2024
To cite this paper please use the final published version:
DOI: 10.1007/978-3-031-63783-4_24

$$(\Delta u_h^{(0)}, \Delta u_\perp) = 0. \tag{17}$$

Under conditions (15) $\Delta u_\perp = w_i \Delta \tilde{u}_h^{(i)}$. We assume the existence of $\Delta u_\perp$ due to Eq. (11).

We search for weights $\{w_i\}$ that ensure the orthogonality condition in the variational statement

$$\{w_i\} = \arg\min(\varepsilon(\vec{w})), \tag{18}$$

$$\varepsilon(\vec{w}) = (\Delta u_h^{(0)}, w_i \Delta u_h^{(i)})^2 / 2. \tag{19}$$

The gradient of expression (19) has the appearance

$$\nabla \varepsilon_k = \frac{\partial \varepsilon}{\partial w_k} = (\Delta u_h^{(0)}, (w_i \Delta u_h^{(i)})) \cdot (\Delta u_h^{(0)}, \Delta u_h^{(k)}). \tag{20}$$

The steepest descent is used for the calculation of weights $\{w_i\}$

$$w_k^{n+1} = w_k^n - \tau \nabla \varepsilon_k. \tag{21}$$

In order to avoid the shift of the exact solution the normalization is used past the termination of iterations

$$\tilde{w}_k^{n+1} = w_k^{n+1} / S^{n+1}, \tag{22}$$

$$S^{n+1} = \sum_{i=1}^{N} w_k^{n+1}. \tag{23}$$

The angle between $\Delta u_\perp$ and $\Delta u_h^{(0)}$

$$\varphi = \arccos\left(\frac{(\Delta u_h^{(0)}, w_i \Delta u_h^{(i)})}{\left|\Delta u_h^{(0)}\right| \cdot \left|w_i \Delta u_h^{(i)}\right|} \right) \tag{24}$$

is used as the orthogonality criterion applied to check the quality of numerical results (convergence of iterations (Eq. (21)).

The basis $\Delta u_h^{(i)} = A_h^{-1} \delta u_h^{(i)} = u_h^{(i),corr} - u_h^{(i)}$ contained from 2 to 5 vectors in numerical tests. The estimation of $\Delta u_h^{(i)}$ at first step of the algorithm is similar to the

ICCS Camera Ready Version 2024
To cite this paper please use the final published version:
DOI: 10.1007/978-3-031-63783-4_24

defect correction approach. However, the expression $u_{\perp} = w_i u_h^{(i)}$ contains the superposition of true approximation errors. We apply only angles between approximation errors $\Delta u_h^{(i)} = A_h^{-1} \delta u_h^{(i)}$ obtained by the defect correction and we search not for the refined solution, but for the hypersphere, containing the projection of true solution on the selected grid. We use the ensemble of $N+1$ numerical solutions. In order to enhance the reliability we consequently select a solution from the ensemble and define it as the basic solution (centre) $C_h = u_h^{(0)}$. After this we estimate the radius $R = \left\| u_h^{(0)} - u_{\perp} \right\|$. Finally, we select the maximum radius and the corresponding centre point over all tries as the solution in the Prager&Synge sense.

4.3. Nonintrusive option for estimation of Prager&Synge solution

The inequalities similar to the Eqs. (5) and (14) are obtained in [13,21,22] (triangle inequality) and [14] (width of ensemble). These approaches may be treated as some approximations of the Prager&Synge method, since the distance between solutions is used as the majorant of error, which circumstance is valid for errors that are close to orthogonal. Unfortunately, the approximation errors $\Delta u_h^{(k)}$ are correlated near discontinuities (the errors involve waves with the positive and negative parts) and, by this reason, are not exactly orthogonal. In several cases the lack of the rigorous orthogonality may be compensated by some additional information. As such information we consider, herein, the maximum distance (ensemble width) between solutions over the ensemble of N independent solutions

$$d_{\max} = \max_{i,k} \left\| u^{(k)} - u^{(i)} \right\| i,k = 1,...,N \tag{25}$$

and assume

$$\left\| \Delta u^{(k)} \right\| \le d_{\max} . \tag{26}$$

The numerical tests by [14] confirm that the inequality (26) becomes more reliable as the number of the ensemble elements increases. So, the estimation of the width of the ensemble (Eq. (25)) and inequality (26) may be considered as some approximation of the Prager&Synge solution.

5 Test problem and numerical algorithms

The above considered methods for the estimation of the Synge solution (*a posteriori* error estimation) are verified by the numerical tests. The numerical solutions for the Euler equations

ICCS Camera Ready Version 2024
To cite this paper please use the final published version:
DOI: 10.1007/978-3-031-63783-4_24

$$\frac{\partial \rho}{\partial t}+\frac{\partial(\rho U_k)}{\partial x_k}=0,$$
$$\frac{\partial(\rho U_i)}{\partial t}+\frac{\partial(\rho U_k U_i+P\delta_{ik})}{\partial x_k}=0,$$
$$\frac{\partial(\rho E)}{\partial t}+\frac{\partial(\rho U_k h_0)}{\partial x_k}=0,$$

describing the flow of the inviscid compressible fluid, are used. The system is two-dimensional, $h_0=(U_1^2+U_2^2)/2+h$, $h=\gamma e$, $E=(e+(U_1^2+U_2^2)/2$ are enthalpy and energies, $P=\rho RT$ is the state equation, $\gamma=C_p/C_v$ is the specific heats relation.

The Edney-I and Edney-VI flow structures [15] are analyzed due to the existence of analytical solutions used for the estimation of the "exact" discretization error $\Delta\tilde{u}^{(k)}=u^{(k)}-\tilde{u}_h$. This error is obtained by the subtraction of the numerical solution from the projection of the analytical one onto the computational grid. Fig. 2 provides the spatial density distribution for Edney-I flow pattern ($M=4$, flow deflection angles $\alpha_1=20^o$ (upper) and $\alpha_2=15^o$ (lower)). Fig. 3 provides the density distribution for Edney-VI ($M=3.5$, angles $\alpha_1=15^o$ and $\alpha_2=25^o$). Figs. 2 and 3 illustrate two patterns for the interaction of two shock waves (inflow at left boundary). The pattern by Fig. 2 corresponds crossing shocks, the pattern by Fig. 3 corresponds two merging shocks.

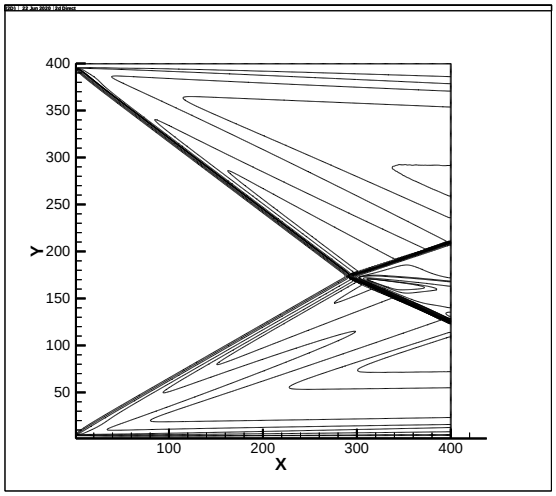

Fig. 2. Density isolines for Edney I flow structure

ICCS Camera Ready Version 2024
To cite this paper please use the final published version:
DOI: 10.1007/978-3-031-63783-4_24

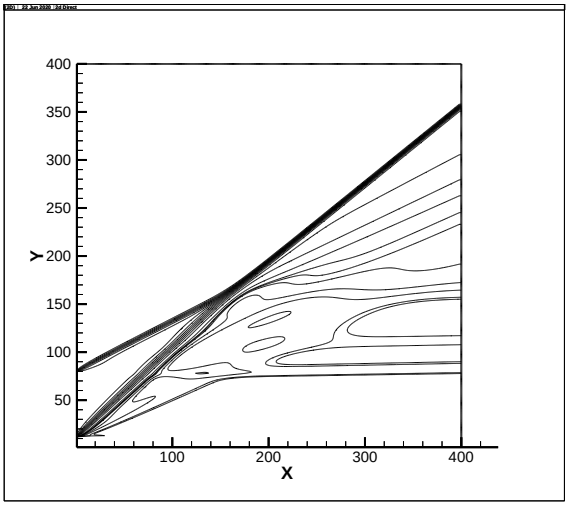

Fig. 3. Density isolines for Edney VI flow structure

We analyze the set of numerical solutions obtained by the numerical methods covering the range of approximation order from one to four. The methods are used that follow. First order algorithm by Courant-Isaacson-Rees [23], second order MUSCL based algorithm that uses approximate Riemann solver by [24], second order relaxation based algorithm [25], third order algorithm based on the modification of Chakravarthy-Osher method [26], fourth order algorithm by [27], second order algorithm by [28].

6 The results of numerical tests

The quality of *a posteriori* error estimation is described by the effectivity index

$$I_{eff} = \frac{\|\Delta u_h\|}{\|\Delta \tilde{u}_h\|}. \tag{27}$$

The condition for existence of the Prager&Synge solution is related with the efficiency index by the inequality $I_{eff} \geq 1$. The relation $3 > I_{eff} \geq 1$ is stated by [7] for the finite-element applications, which imply sufficiently smooth solutions.

We performed numerical experiments for several cases including different flow structures (Edney-I, Edney-VI), different flow parameters (Mach numbers in the range $3 \div 5$, shock angles in the range $10 \div 30^o$) and uniform grids of 100×100, 200×200 and 400×400 nodes. Below several typical results are presented as the illustrations of different methods for calculation of the Prager&Singe solution.

ICCS Camera Ready Version 2024
To cite this paper please use the final published version:
DOI: 10.1007/978-3-031-63783-4_24

The truncation error based estimation (Eqs. (8)-(14)) provides nonrealistic pessimistic results for the efficiency index $I_{eff} \sim 10 \div 20$. In combination with the extremely algorithmic complexity these results make this option non competitive.

The approximation error based estimation (Eqs. (15)-(24)) provides acceptable results.

The results provided by nonintrusive option (Eq. (25),(26) are close in the values of the efficiency index to results obtained by the approximation error based estimation (Eqs. (15)-(24)).

Herein, we consider the numerical tests for the algorithm described in the Section 4.2 and based on the superposition of independent numerical solutions. The Edney-VI shock interaction pattern ($M = 3.5$, $\alpha_1 = 15^o$, $\alpha_2 = 25^o$) was used for the numerical tests on the grids containing 100×100 and 400×400 nodes.

At first step the solution obtained by the method [24] is used as the basic solution $u_h^{(0)}$, which is considered as the centre of the hypersphere containing the true solution (more correctly, the projection of the true solution on considered grid). The additional solutions $u_h^{(1)}$ [23], $u_h^{(2)}$ [26], $u_h^{(3)}$ [27], $u_h^{(4)}$ [28], $u_h^{(5)}$ [25] are used in different combinations in order to generate some orthogonal error and the superposition of solutions as the approximation of the auxiliary solution $u_\perp = w_i u_h^{(i)}$.

The value $R = \left\| u_h^{(0)} - u_\perp \right\|$ is the radius of the hypersphere with the centre $C_h = u_h^{(0)}$, which contains the true solution

First, two solutions ($u_h^{(1)}$ [23], $u_h^{(2)}$ [26],) are used to determine the radius of the hypersphere. The weight values are $w_1 = -0.790$, $w_2 = 1.79$, the value of the angle between $\Delta u_\perp$ and $\Delta u_h^{(0)}$, $\varphi = 87.6$. The true error norm, Prager&Synge estimates of error norm and the efficiency index having the form $I_{eff} = \left\| u_h^{(0)} - u_\perp \right\| / \left\| u_h^{(0)} - \tilde{u} \right\|$ are provided in the Table 1.

Table 1. True error norm, error norm estimation and efficiency index

$\left\| u_h^{(0)} - \tilde{u} \right\|$	$\left\| u_h^{(0)} - u_\perp \right\|$	I_{eff}
0.114	1.115	9.780

Second, three solutions ($u_h^{(1)}$ [23], $u_h^{(2)}$ [26], $u_h^{(3)}$ [27]) are used. The weight values are $w_1 = -0.579$, $w_2 = 0.654$, $w_3 = 0.925$, the angle $\varphi = 90.0$ and $I_{eff} = 3.38$.

ICCS Camera Ready Version 2024
To cite this paper please use the final published version:
DOI: 10.1007/978-3-031-63783-4_24

Third, four solutions ($u_h^{(1)}$ [23], $u_h^{(2)}$ [26], $u_h^{(3)}$ [27], $u_h^{(4)}$ [28]) are used. The corresponding weights are: $w_1 = -0.415$, $w_2 = 0.315$, $w_3 = -0.475$, $w_4 = 0.624$, the angle $\varphi = 89.9^o$ and $I_{eff} = 1.741$.

Fourth, five solutions ($u_h^{(1)}$ [23], $u_h^{(2)}$ [26], $u_h^{(3)}$ [27], $u_h^{(4)}$ [28], $u_h^{(5)}$ [25]) are used. The corresponding weights are: $w_1 = -0.453$, $w_2 = 0.239$, $w_3 = 0.391$, $w_4 = 0.532$, $w_5 = 0.290$, angle $\varphi = 89.8^o$ and $I_{eff} = 1.438$.

At the next steps all other numerical solutions are consequently selected as the basic solution $u_h^{(0)}$ and the radius $R = \left\| u_h^{(0)} - u_\perp \right\|$ is computed.

The numerical tests on the grids containing 400×400 nodes are performed in order to study the influence of the mesh step on results.

The minimum value the effectivity index over all tests was greater the unit that confirms the successive estimation of the Prager&Synge solution.

The maximum value the effectivity index over all basic solutions is presented by the Table 2 in the dependence on the number of additional solutions for two different grids.

Table 2. The efficiency index in dependence on the number of solutions

N of solutions	2	3	4	5
$I_{eff}\,(100 \times 100)$	10.810	3.680	1.931	1.583
$I_{eff}\,(400 \times 400)$	9.081	1.754	1.437	1.329

One may see from the Table 2 that the magnitude of the effectivity index decreases as the number of solutions in use is enhanced. In general, two auxiliary solutions provide too pessimistic estimations of the approximation error. In the range of 3-5 solutions the values of the effectivity index are quite acceptable. Some saturation of the effectivity index is observable at increasing of the number of solutions. The grid resolution rather weakly affects the effectivity index.

In general, the numerical tests demonstrate the following situation.

The version of the Prager@Synge method based on the adjoint postprocessor and the defect correction (Eqs.(8-14))) overestimates the error and provides the effectivity index in the range $I_{eff} \sim 10 \div 20$ that is too pessimistic.

The version of the Prager@Synge method based on the superposition of solutions (Eq. (15)) provides the effectivity index in the range $I_{eff} \sim 1.3 \div 3.7$.

ICCS Camera Ready Version 2024
To cite this paper please use the final published version:
DOI: 10.1007/978-3-031-63783-4_24

The effectivity index, based on the ensemble width (Eq. (26)), is in the range $I_{eff} \sim 1.1 \div 2.5$ for the considered ensemble of numerical solutions engendered by six algorithms.

7 Conclusion

The original concept of the numerical solution is the main idea of the Prager&Synge method. This solution is not based on asymptotics at grid step diminishing and enables to avoid the modern “tyranny" of mesh refinement. Instead of the sequence of solutions, occurring at the grid size diminishing, the Prager&Synge solution deals with the hypersphere containing the projection of the true solution on a computational grid. The numerical solution is the centre of this hypersphere. The Prager&Synge solution provides a natural way to *a posteriori* error estimation and natural criterions for the mesh refinement termination related with the required tolerance of valuable functionals.

The limited domain of application is the main drawback of the Prager&Synge method in the original form. The universal versions of Prager&Synge method that may by applied to an arbitrary PDE system are discussed. They include intrusive and nonintrusive options for the calculation of the Prager&Synge numerical solution.

The intrusive version is based on the superposition of numerical solutions and is specified by the moderate complexity of the algorithm.

The nonintrusive version (based on the width of ensemble) is some approximate variant of the intrusive version with the minimum complexity of the algorithm.

These approaches to the computation of the numerical solution in the sense of the Prager&Synge are compared for the two dimensional compressible flows with the shock waves and demonstrated the acceptable value of efficiency index for the error norm estimation.

References

1. Guide for the Verification and Validation of Computational Fluid Dynamics Simulations, American Institute of Aeronautics and Astronautics, AIAA-G-077-1998, VA (1998)
2. Standard for Verification and Validation in Computational Fluid Dynamics and Heat Transfer, ASME V&V 20-2009 (2009)
3. Prager, W., Synge, J. L.: Approximation in elasticity based on the concept of function spaces, Quart. Appl. Math. 5 241-269 (1947)
4. Synge J.L.: The Hypercircle in Mathematical Physics, CUP, London, (1957)
5. Synge J.L.: The Hypercircle method, In Studies in Numerical Analysis, Academic Press, London, p. 201-217 (1974)
6. Babuska, I., Rheinboldt, W.: A posteriori error estimates for the finite element method. Int. J. Numer. Methods Eng. 12, 1597–1615. (1978)
7. Repin, S.I.: A posteriori estimates for partial differential equations. Vol. 4. Walter de Gruyter (2008)

ICCS Camera Ready Version 2024
To cite this paper please use the final published version:
DOI: 10.1007/978-3-031-63783-4_24

8. Ainsworth, M., Oden, J. T.: A Posteriori Error Estimation in Finite Element Analysis. Wiley, NY. (2000)
9. Richardson, L. F.: The Approximate Arithmetical Solution by Finite Differences of Physical Problems Involving Differential Equations with an Application to the Stresses in a Masonry Dam, Trans. of the Royal Society of London, Series A, V. 2 10, pp. 307–357. (1908)
10. Alexeev, A.K., Bondarev, A.E.: On Some Features of Richardson Extrapolation for Compressible Inviscid Flows. Mathematica Montisnigri, XL, 42–54. (2017)
11. Roy, Ch. J.: Grid Convergence Error Analysis for Mixed-Order Numerical Schemes, AIAA Journal, 41(4) 595-604. (2003)
12. Carpenter, M. H., Casper, J.H.: Accuracy of Shock Capturing in Two Spatial Dimensions, AIAA J., 37(9) 1072-1079. (1999)
13. Alekseev, A.K., Bondarev, A.E., Navon, I. M.: On Triangle Inequality Based Approximation Error Estimation, arXiv:1708.04604, (2017)
14. Alekseev, A.K., Bondarev, A. E., Kuvshinnikov, A. E.: On Uncertainty Quantification via the Ensemble of Independent Numerical Solutions, Journal of Computational Sci., 42, 10114 (2020)
15. Edney, B.: Effects of Shock Impingement on the Heat Transfer around Blunt Bodies. AIAA J., 6(1) 15-21. (1968)
16. A. K. Alekseev, A. E. Bondarev, The Numerical Solution in the Sense of Prager&Synge, arXiv: 2403.06273, (2024)
17. Alekseev, A.K., Bondarev, A.E.: On a posteriori error estimation using distances between numerical solutions and angles between truncation errors, Mathematics and Computers in Simulation, Volume 190, Pages 892-904 (2021)
18. Shokin, Yu. I.: Method of differential approximation. Springer-Verlag, (1983)
19. Alekseev, A.K., Navon, I.M.: A Posteriori Error Estimation by Postprocessor Independent of Flowfield Calculation Method, Computers & Mathematics with Applications, v. 51, 397-404. (2006)
20. Linss, T., Kopteva, N.: A Posteriori Error Estimation for a Defect-Correction Method Applied to Convection-Diffusion Problems, Int. J. of Numerical Analysis and Modeling, V. 1, N. 1, 1–16. (2009)
21. Alekseev, A.K., Bondarev, A.E.: Estimation of the Distance between True and Numerical Solutions, Computat. Mathematics and Math. Physics, V. 59, N. 6, 857–863. (2019)
22. Alekseev, A.K., Bondarev, A. E.: On A Posteriori Estimation of the Approximation Error Norm for an Ensemble of Independent Solutions, Numerical Analysis and Appl., 13(3), 195-206 (2020)
23. Courant, R., Isaacson, E., Rees, M.: On the Solution of Nonlinear Hyperbolic Differential Equations by Finite Differences, Comm. Pure Appl. Math. V. 5. 243-255 (1952)
24. Sun, M., Katayama K. An artificially upstream flux vector splitting for the Euler equations, JCP. V. 189. 305-329 (2003)
25. Trac, Hy, Pen, Ue-Li: A Primer on Eulerian Computational Fluid Dynamics for Astrophysics, arXiv:0210611v2, (2002)
26. Osher, S., Chakravarthy, S.: Very high order accurate TVD schemes, ICASE Report. N. 84-144. 229–274 (1984)
27. Yamamoto, S., Daiguji, H.: Higher-order-accurate upwind schemes for solving the compressible Euler and Navier-Stokes equations, Computers and Fluids. V. 22. 259-270 (1993)
28. MacCormack, R. W.: The Effect of Viscosity in Hypervelocity Impact Cratering, AIAA Paper 69-354, (1969)

ICCS Camera Ready Version 2024
To cite this paper please use the final published version:
DOI: 10.1007/978-3-031-63783-4_24